Aerosol and Air Quality Research, 17: 2491–2508, 2017

ISSN: 1680-8584 print / 2071-1409 online
doi: 10.4209/aaqr.2017.01.0009

An Integrated WRF-CAMx Modeling Approach for Impact Analysis of Implementing the Emergency $PM_{2.5}$ Control Measures during Red Alerts in Beijing in December 2015

Jia Jia[1], Shuiyuan Cheng[1,2*], Lei Liu[3], Jianlei Lang[1], Gang Wang[1], Guolei Chen[1], Xiaoyu Liu[1]

[1] *Key Laboratory of Beijing on Regional Air Pollution Control, Beijing University of Technology, Beijing 100124, China*
[2] *Collaborative Innovation Center of Electric Vehicles in Beijing, Beijing 100081, China*
[3] *Department of Civil and Resource Engineering, Dalhousie University, Halifax, NS B3H 4RZ, Canada*

ABSTRACT

In December 2015, the Beijing-Tianjin-Hebei (BTH) region experienced several episodes of heavy air pollution. Beijing municipal government therefore issued 2 red alerts on December 7 and 19, respectively, and also implemented emergency control measures to alleviate the negative effects of pollution. It is estimated that the heavy pollutions in 2 red alert periods in Beijing were due mainly to the accumulation of air pollutants from local emission sources and the transboundary transport of pollutants from surrounding areas. The collected meteorological and $PM_{2.5}$ data indicate that the severity of air pollutions were enlarged by the poor meteorological conditions along with lower mixing layer height. In this study, the WRF-CAMx modeling system was utilized not only for analyzing the contributions of $PM_{2.5}$ from different sources, but also for quantitatively assessing the effects of implementing various emergency control measures on $PM_{2.5}$ pollution control during the red alert periods. The modeling results show that local emissions were the most dominant contributors (64.8%–83.5%) among all emission sources, while the main external contributions came from the city of Baoding (3.4%–9.3%). In addition, among 5 different emission source categories, coal and traffic were the two dominant contributors to $PM_{2.5}$ concentration in urban area of Beijing. Then four pollution control scenarios were designed particularly to investigate the effectiveness of the emergency control measures, and the results show that, generally these emergency control measures have positive effects on air pollution reduction. In particular, restrictive measures of traffic volume control and industrial activity shutdown/suspension have been found as the most effective measures in comparison to other emergency control measures. It is recommended that such effective measures should be considered to implement when next time similar heavy air pollutions occur in the city of Beijing.

Keywords: Integrated WRF-CAMx modeling; Red alerts; Emergency control measures; Beijing.

INTRODUCTION

As the political and cultural center of China, Beijing has made and implemented an ambitious urban development plan over the past two decades to transform an old and historical city to a new and modern metropolis (Dong *et al*., 2013). Beijing has gradually achieved its goal in terms of its stunning infrastructural construction and sweeping architectural transformation. Examples of such progresses and milestones include the successful holds of Beijing Olympic Summer Games in 2008 and APEC (Asia-Pacific Economic Cooperation) Beijing Summit in 2014, during which Beijing has acquired the moment and spotlight in front of thousands visiting China and billions watching on television.

However, associated with its rapid urban transformation and economic expansion, air quality in Beijing's urban areas has been severely deteriorated by elevated levels of smog and other air toxins. Among all the air pollutants, $PM_{2.5}$ pollution was prompted and became the topmost pollution related priority for Beijing municipal government (Zhang *et al*., 2015b). The harmful consequences of high levels of $PM_{2.5}$ in the air are obvious and substantial in terms of negative impacts on urban environmental, economic development and public health (Feng *et al*., 2014b; Guo *et al*., 2014; Zhou *et al*., 2014b; Jiang *et al*., 2015). As a result, Beijing government desires to take effective strategies and policies to control the level of $PM_{2.5}$ concentration in the air to improve the environmental performance, and eventually provide healthy and clean air for its own residents.

* Corresponding author.
Tel.: +86 10 67391656; Fax: +86 10 67391983
E-mail address: bjutpaper@gmail.com

The urban air quality system is a complex network of multiple competing interactions within and among chemical and physical atmospheric processes, which is also related to various social, economic, environmental, technological, managerial, regulatory, and political factors. Hence, the decision making process of air quality management thus requires an insightful knowledge of air pollution details and a sound understanding of the significant drivers of urban air pollution problems.

Since two decades ago, the Central Government of China has made extensive efforts (including emergency control measures for important events) to alleviate the emission in both Beijing and its surrounding provinces for improving the air quality and positive results have been achieved. For example, during the aforementioned international events (i.e., 2008 Beijing Olympic Games (Wang *et al*., 2009; Wang *et al*., 2014b), 2014 APEC Summit (Chen *et al*., 2015b)), massive emission control measures were designed collectively by the governments of Beijing and surrounding provinces, and more importantly, were implemented a few weeks prior to the events; as a result, the air quality of Beijing was generally improved to good conditions and the $PM_{2.5}$ concentrations were at low levels. Although these measures seemed to have positive effects on air quality improvement, it has to be recognized that, both Olympics and APEC Summit events were held in summer and autumn seasons in Beijing, and the weather conditions were often favorable for dispersing and pushing the polluted air out of the Beijing airshed (Wang *et al*., 2010; Huang *et al*., 2015).

In December 2015, the Beijing-Tianjin-Hebei (BTH) region experienced several episodes of heavy air pollution, and each episodes lasted for a few days. The maximum instantaneous $PM_{2.5}$ concentration in Beijing reached over 600 μg m^{-3}, which was the highest level since January 2013 (Bi *et al*., 2014). As a quick and emergency response to pollution situations, Beijing municipal government therefore issued 2 red alerts on December 7 and 19, respectively, and emergency control measures were implemented immediately to control the pollution and help alleviate the negative effects of pollution. This was the first time that a red alert for air pollution in Beijing was issued since the Emergency Air Pollution Response System (Response System) was announced in 2013 (Chen *et al*., 2015a). Previous studies indicate that the effectiveness of emergency control measures for improving air quality in Beijing was influenced by not only air pollutant reductions at emission sources but also the regional weather conditions (Yang *et al*., 2015b). Hence, whether or not the emergency control measures are effective or how much effects they could achieve in alleviating air pollution without favorable meteorological conditions became doubtful and are unknown to the governmental authorities, and they needs to be investigated particularly for Beijing in winter seasons when the heavy air pollutions occur quite frequently and the weather conditions are often not favorable in pollution dispersion.

To investigate the effectiveness of emission control measures under different complex terrain and meteorological conditions like Beijing, two different types of modeling approaches were used in the past, including receptor models and numerical models. Receptor models use the observed data to compare the composition changes of primary and secondary aerosols in the air before and after the implementation of emergency control measures (Xing *et al*., 2011; Wei *et al*., 2014; Wang *et al*., 2015b; Yan *et al*., 2015); numerical models use emission inventories to specify the source regions and the efficiency and effectiveness of control measures can be assessed through simulating different control scenarios. Previously, a Community Multi-Scale Air Quality (CMAQ) numerical simulation model has been applied to the BTH region and the modeling results show that the emergency control measures have relatively significant effects on reducing NO_x and SO_2 concentrations, but limited impacts on $PM_{2.5}$ pollution control (Chen *et al*., 2015a). It was found that the zero-out method used in the CMAQ model couldn't provide accurate appointments of $PM_{2.5}$ sources due to the complex non-linearity of atmospheric chemistry. In order to overcome this drawback, the Comprehensive Air Quality model with Extensions (CAMx) has then been developed for better $PM_{2.5}$ pollution simulation. CAMx is an Eulerian (gridded) regional photochemical dispersion model, which could simulate the emission, dispersion, chemical reaction, and removal of pollutants by marching the Eulerian continuity equation forward in time for each chemical species on a system of nested three-dimensional grids. In CAMx, the Particulate Source Appointment Technology (PSAT), an efficient source tagging method (Li *et al*., 2015b), is employed as the source apportionment method to accurately reflect the pollutant transmission and appointment of sources at a regional scale, the effectiveness of emission control measures can also be investigated (Shen *et al*., 2011; Wang *et al*., 2014a; Qu *et al*., 2014; Koo *et al*., 2015; Li *et al*., 2015b; Pirovano *et al*., 2015). For example, Megaritis *et al*. (2014) applied CAMx model to Europe to study the influence of emissions changes on fine PM levels, with the result was that reduction of NH_3 emissions seems to be the most effective control strategy for reducing $PM_{2.5}$ over Europe. Akritidis *et al*. (2014) used the CAMx modeling system to assess the impact of anthropogenic emission changes on air quality improvement in Europe and pointed out that any gain owning to emissions changes in short time periods can be masked by meteorological and background ozone variabilities. Li *et al*. (2013) applied the CAMx model to a study on the contributions of various precursors to air pollution formation, and found that regional collaborations on pollution control are of particular importance in effectively reducing the episodic ozone concentrations. Li *et al*. (2015b) further employed the CAMx model to a study on the contributions of different emission sources and regions to $PM_{2.5}$ level in the BTH region in 2006 and 2013, respectively, and found that the emission control measures and particularly regional joint emission control efforts could help achieve much better pollution control results.

As an extension of previous efforts in this area, in this study, the CAMx modeling system is used for the first time to simulate the regional air quality system in BTH region during 2 red alert periods and answer various questions relating to $PM_{2.5}$ pollution occurred in Beijing. This mainly

entails: (1) how the heavy air pollution was formed in December 2015, especially in 2 red alert periods in Beijing? (2) how did the meteorological conditions influence the formation of heavy air pollution in December 2015? (3) what percentages did different emission sources and sub-regions contribute to the formation of $PM_{2.5}$ pollution in Beijing in 2 red alert period? (4) how effective did the emergency control measures perform in improving the air quality in Beijing and which one is most effective and preferred? The heavy air pollution episodes occurred in December 2015 in Beijing provide a rare and valuable opportunity not only for testing the capability of the CAMx modeling system in simulating regional large-scale air quality problem, but also for examining the effects of various emergency control measures on air pollution control. The modeling results would provide a scientific base for Beijing's government to make more sound air pollution control policies and measures in future.

CASE STUDY

Two Red Alerts Issued in December 2015

According to the Heavy Air Pollution Emergency Response Program stipulated by Beijing municipal government, four colors (i.e., blue, yellow, orange and red) are used as a 4-tier alert system to indicate the severity levels of air pollution in the city, and the color of alert will be based on the comprehensive forecasting of the degree and duration of air pollution. Among four colors, blue, yellow, and orange alerts are issued for the conditions that a heavy air pollution is predicted to continue for 24 hours, 48 hours, and 72 hours, respectively. Whereas, the red alert will be issued for a forecasted heavy pollution that would last over 72 hours, and represents the highest level of alert, as indicated in Table 1. Table 1 presents the issuing conditions for the 4-tier alerts as well as their corresponding control measures for protecting air and public health. The control measures could be divided into three groups, i.e., public health protection measures, recommended control measures, and compulsory control measures. As long as a heavy pollution occurs, these public health protection measures will be brought to public notice for raising their awareness and protecting themselves. Recommended measures are designed to reduce personal emissions through, for example, reducing the usage of private vehicles and instead using more public transit. The yellow, orange and red alerts all include a variety of compulsory measures which will be implemented for reducing pollutant emissions from a variety of major sources such as vehicles, industrial plants and construction sites and thus possibly alleviating the $PM_{2.5}$ pollution in the city.

On December 7, 2015, the $PM_{2.5}$ concentrations observed from almost all monitoring stations across Beijing were more than 200 μg m^{-3}, and Beijing Municipal Environmental Monitoring Center predicted that a heavy air pollution with a $PM_{2.5}$ concentration of over 150 μg m^{-3} would continue for more than three consecutive days, before the arrival of the northwest cold winds which might be able to help pollution disperse away. As a result, a red alert was issued

Table 1. The issuing conditions for the 4-Tier alerts and the corresponding control measures.

Alert Level	Issuing Conditions	Control Measures		
		Public Health Protection Measures	Recommended Measures	Compulsory Measures
Blue	Mean hourly $PM_{2.5}$ concentration over 150 μg m^{-3} lasting 24 hours	1. Reduce outdoor activities 2. Public warning and notification	1. Clean roads 2. Reduce usage of vehicles	
Yellow	Mean hourly $PM_{2.5}$ concentration over 150 μg m^{-3} lasting over 24 but less than 48 hours	1. Avoid outdoor activities 2. Public warning and notification	1. Reduce usage of vehicles 2. Cancel outdoor sports activities for all schools	1. Ban partial activities of construction projects 2. More road cleaning
Orange	Mean hourly $PM_{2.5}$ concentration over 150 μg m^{-3} lasting over 48 but less than 72 hours	1. Avoid outdoor activities 2. Expert interpretation and information publicity 3. Wear masks	1. Reduce usage of vehicles 2. Cancel all outdoor activities for all schools	1. More road cleaning 2. Enhanced dust control of construction sites 3. Suspend the operation of some industrial plants 4. Ban fireworks and outdoor barbecues 5. Ban heavy vehicles on road
Red	Mean hourly $PM_{2.5}$ concentration over 150 μg m^{-3} lasting over 72 hours	1. Avoid outdoor activities 2. Expert interpretation and information publicity 3. Wear masks	1. Cancel all large outdoor activities 2. Close all schools	1. Implement even- and odd-numbered license plates policy 2. Ban heavy-duty vehicles on road 3. Suspend all construction projects 4. Suspend the operation of more industrial plants 5. Ban fireworks and outdoor barbecues

by Beijing municipal government at 7:00 AM on December 8; meanwhile the emergency control measures were put into implementation immediately in Beijing. Furthermore, according to the estimation made by Beijing Environmental Protection Bureau, 28%–36% of total $PM_{2.5}$ in Beijing's airshed came from the transboundary emissions from neighboring provinces (Wang *et al*., 2015a), particularly from Hebei Province and the City of Tianjin. In order to help mitigate the severity of air pollution level in Beijing, the surrounding provinces and cities responded quickly and have taken collective responsibilities and actions through issuing different levels of alerts and implementing various control measures. For example, the city of Baoding issued a red alert; the city of Tianjin issued an orange alert; and the city of Qinhuangdao issued a blue alert on the same day of December 7. This first red alert in Beijing was cancelled till 12:00 PM on December 10 along with the improvement of air quality in Beijing. The red alerts were issued at 7:00 AM on December 19, 2015 by the governments of Beijing municipality, Tianjin city and Hebei province due to the recurrence of high $PM_{2.5}$ concentrations in this region, and they were cancelled till 24:00 AM on December 22 where the air quality was much improved in the region. Fig. 1 shows the different levels of alerts issued for different cities and regions in December 2015. As mentioned earlier, although the red alerts were issued in the region and various emergency control measures were implemented, the effectiveness of these measures on regional air quality improvement remains to be unknown and deserves an insightful research on this issue.

Data Collection

In this study, meteorological parameters and hourly concentrations of different air pollutants (including $PM_{2.5}$, SO_2, NO_2, O_3, and CO) were collected from the field monitoring stations located in the study region. Meteorological parameters are used to analyze the impacts of meteorological conditions on the air quality in the study region during the red alert periods. Air pollutant concentrations are used not only for the validation of the CAMx air quality simulation model but also for the trend analysis of $PM_{2.5}$ concentrations. The hourly concentrations of air pollutants were collected by China National Environmental Monitoring Centre (CNEMC) for the period of December 2013 to December 2015. The mean values of state-controlled monitoring stations in Beijing (12 sites in Beijing-Urban), Tianjin, Shijiazhuang and Tangshan are utilized to calculate the $PM_{2.5}$ concentrations, respectively. Meteorological data used in this study include temperature, relative humidity, visibility, wind direction and wind speed, and they are available on the China Weather Website which are collected by China Meteorological Bureau and Weather Underground. Surface meteorological maps are obtained from the Korea Meteorological Administration (KMA), and they are analyzed to identify the dominant synoptic features of different weather patterns during the 2 red alert periods. In addition, the daily maximum layer height (MLH) is calculated by the dry adiabatic method through using the daily maximum temperatures data drawn by Aircraft Meteorological Data Relay (AMDAR) from Beijing Capital International Airport (40°04′N, 116°35′E), which is located 25 km to the northeast of metro center of Beijing.

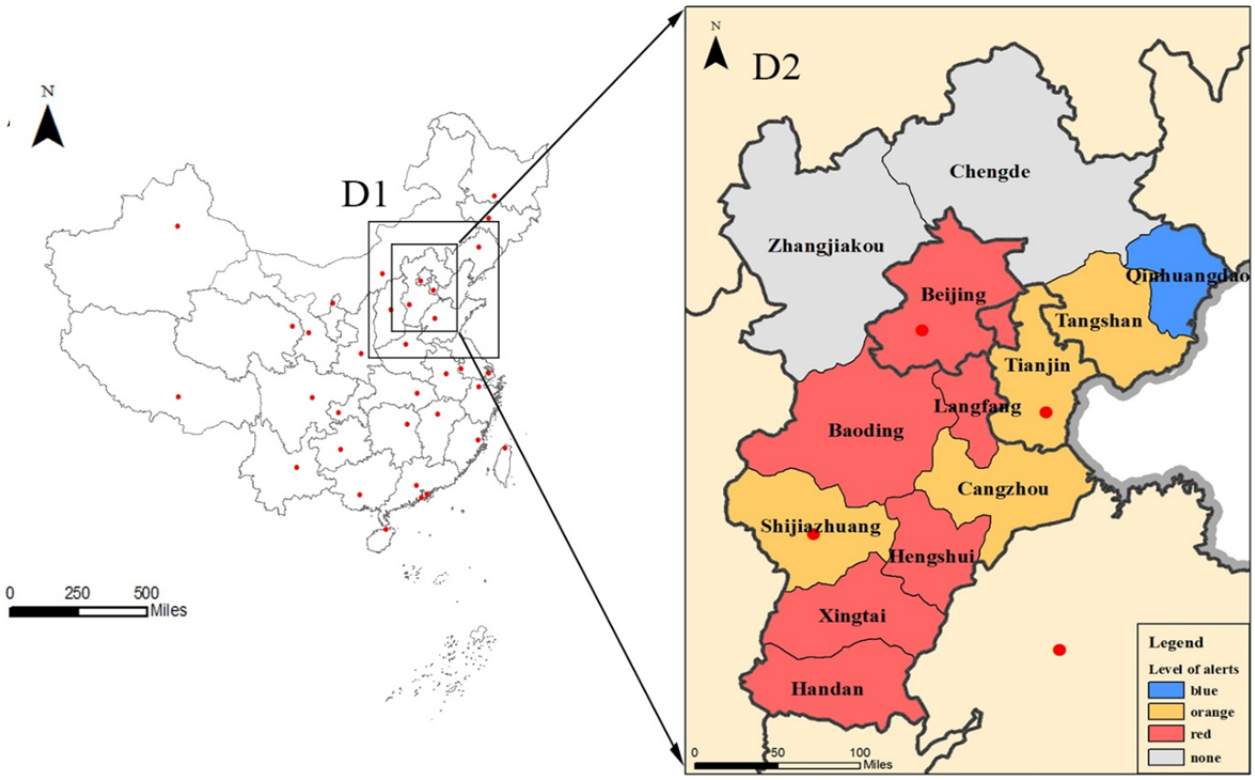

Fig. 1. Designed double nesting simulation domain and different alerts issued in December 2015.

WRF-CAMx Modeling System

Methodology Design

In this study, an integrated WRF-CAMx modeling system is used as the tool to investigate the effects of various emergency control measures on air pollution control. The WRF stands for the Weather Research & Forecasting Model (Version 3.3), and it was developed by the National Center for Atmospheric Research (NCAR). Its role is to generate the meteorological background for air quality simulation. In the WRF meteorological simulation, the Final Operational Global Analyses data are used, which were produced by National Centers for Environmental Prediction's (NCEP) Global Forecast System (GFS). In the WRF-CAMx modeling system, the CAMx model (Version 5.1) is an advanced photochemical diffusion model based on the framework of 'one atmosphere'. In this study, the CAMx model is employed to simulate the spatial and temporal variations of $PM_{2.5}$ concentrations within the study region. In the process of simulation, the Particulate Source Appointment Technology (PSAT) was used as a source apportionment tool to estimate the contributions from respective emission sources (Wu *et al*., 2013), through adding reactive tracers into the CAMx model to apportion $PM_{2.5}$ components from different sub-regions and source categories. After each chemical or physical process (e.g., chemical reaction, deposition, diffusion and transport), the source species are updated by apportioning the change of corresponding species in the CAMx model to each source. As a result, source information of each selected species on each grid at each time step are delivered and evolved (Li *et al*., 2015b). Detailed CAMx model and PSAT algorithms can be found in the manual of the CAMx model.

Simulation Domain Design

In this study, a double nesting simulation domain was designed for the integrated WRF-CAMx modeling system, as shown in Fig. 1. Domain 1 (D1) refers to the outside domain with a grid resolution of 27 km × 27 km. It covers the BTH region and surrounding provinces including Shandong, Shanxi, most of Inner Mongolia, Liaoning, Shaanxi, Henan, Jiangsu, and parts of Jilin, Anhui, Hubei, with a total area of almost 1.8 million km^2. This design makes all possible external $PM_{2.5}$ emission sources (which might affect the $PM_{2.5}$ concentration in the BTH region) be included in the simulation emission inventory. Domain 2 (D2) refers to the inside domain with a grid size of 9 km × 9 km, and it covers mainly the BTH region. Presumably, D2 provides a better $PM_{2.5}$ simulation resolution.

Pollution Emission Sub-Areas Setup

In the air quality simulation, the simulation domain needs to be divided into a series of sub-areas for evaluating the pollutant transport between geographic boundaries of sub-areas labeled by the CAMx model. In this study, Beijing's urban area and rural area were treated separately due to their significant differences in population density and traffic volume (Wu *et al*., 2013), and they represents two different sub-areas as the inputs for the CAMx model.

In this study, a total of 15 sub-areas were delineated within the D2 domain, representing 15 pollution emission source inputs to the CAMx model, as indicated in Fig. 2. The 15 sub-areas are Beijing-Urban (BJ-U), Beijing-Rural (BJ-R), Tianjin (TJ), Zhangjiakou (ZJK), Chengde (CD), Qinhuangdao (QHD), Tangshan (TS), Baoding (BD), Langfang (LF), Cangzhou (CZ), Shijiazhuang (SJZ), Hengshui (HS), Xingtai (XT), Handan (HD) and other regions (OT). Receptor points were selected close to the state-controlled monitoring stations within TJ, SJZ, TS and BJ-U sub-area to calculate the local simulation $PM_{2.5}$ concentrations and verify the CAMx model, respectively. In addition, the receptors in BJ-U were also used to investigate the pollutant transboundary transport and sources apportionment.

Emission Inventory

The emission inventory was calculated based on raw emissions data, emission coefficients and activity categories, which were directly acquired from provincial or municipal environmental protection bureaus and administration departments. More detailed descriptions of the complete emission inventory which were used in this study could be found in previous works published by the researchers in the Key Laboratory of Beijing on Regional Air Pollution Control (Lang *et al*., 2013b; Zhou *et al*., 2014a). The pollutants in the emission inventory include SO_2, NO_x, PM_{10},

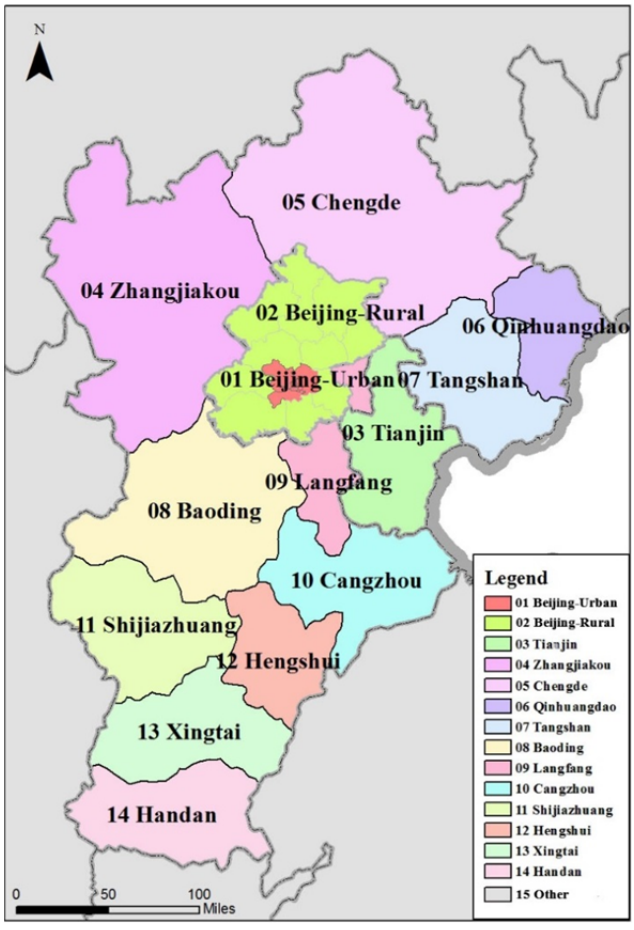

Fig. 2. The 15 sub-areas delineated as the pollution source inputs for the CAMx model.

$PM_{2.5}$, volatile organic compounds (VOCs), and various components in $PM_{2.5}$ and VOCs. In addition, the emission inventory was divided into 5 emission categories, including industrial sources (industry), transportation sources (traffic), coal-burning sources (coal), dust sources (dust) and other sources (others, including biomass burning sources, waste discharge sources, agricultural ammonia emissions sources, etc.). The calculated emission reduction ratios, which were calculated base on the previous experiences (e.g., the reduction ratios of the APEC Summit period which were published on website of the Beijing Municipal Environmental Protection Bureau) and the comparison of control measures in different periods, resulted from the implementation of emergency control measures during the 2 red alert periods in December 2015 were also included to update the emission inventory, as shown in Table 2.

Model Verification

In this study, the simulated $PM_{2.5}$ concentrations were compared to the observed data to validate the model. The indicators for model verification include correlation coefficient (R), normalized mean bias (NMB), normalized mean error (NME), and the fraction (M_i/O_i) satisfying the condition $0.5 \leq M_i/O_i \leq 2$ (FAC), where M_i and O_i are the simulated and observed $PM_{2.5}$ concentration at time i. The statistic approaches used in this study can be found in many previous literatures (Cheng *et al*., 2012; Zhou *et al*., 2012). Fig. 3 presents the comparison results of the simulated and observed $PM_{2.5}$ concentrations for the period of December 7 to 31, 2015 for the sub-areas of BJ, TJ, SJZ and TS. The results indicate that high correlations between observed and simulated concentrations are obtained and the simulation errors are insignificant at an acceptable level. In particular, the value of R is greater than 0.70, with the NMB ranges of –15%–12%, the NME ranges of 33%–38%, and the FAC ranges of 88%–91%. The model validation errors come possibly from three sources: (1) missing or incomplete activity data in the emission inventory; (2) improper or imbalanced implementation of the emergency control measures in different areas leading to errors when calculating the emission reduction ratios; (3) errors from the WRF-CAMx modeling process itself. However, in general, the comparison results indicate that an acceptable agreement between the simulated and observed concentrations has been achieved (Lang *et al*., 2013a; Chen *et al*., 2014; He *et al*., 2014) and the WRF-CAMx modeling system can be utilized for $PM_{2.5}$ concentration simulation and control measure evaluation.

Simulation Scenario Design

In this study, four simulation scenarios were designed in order to quantify the effects of implementing the emergency control measures on $PM_{2.5}$ concentration reduction in the BTH region during the red alert periods. Scenario BASE was designed to represent the actual $PM_{2.5}$ pollution process in Beijing for the 2 red alert periods in December 2015, during which various emergency control measures were implemented immediately after red alerts were issued. The simulation results from Scenario BASE was used for model verification and $PM_{2.5}$ evolution trend analysis. The BASE scenario was also utilized for ranking the relative importance of different emission sub-areas and inventory categories through calculating their specific contributions. Scenario NC (No-Control scenario) was designed to represent the situation which assumes no emergency control measures being implemented in the study region during the 2 red alert periods. The Scenario NC simulation results were used to compare with Scenario BASE results and the difference demonstrates the effectiveness of emergency control measures. Scenario NBC (No-Beijing-Control scenario) was designed to represent the situation that only Beijing areas do not implement any emergency control measures. Scenario NHTC (No-Hebei-Tianjin-Control scenario) represents the situation that Hebei and Tianjin do not implement any emergency control measures. Scenarios NBC and NHTC were designed to evaluate the impacts of emission contributions from Beijing areas and Hebei-Tianjin areas on the level of $PM_{2.5}$ concentration in Beijing urban area.

Table 2. The pollutant emission reduction ratios in the BTH region during red alert periods.

Emission Region	Source Category	SO_2	NO_x	PM_{10}	$PM_{2.5}$	VOC
Beijing	Traffic	-	48%	59%	60%	50%
	Industry	55%	46%	40%	42%	37%
	Dust	-	-	46%	48%	-
	Other[a]	10%	10%	10%	10%	10%
Tianjin	Traffic[b]	-	-	-	-	-
	Industry	30%	30%	30%	30%	30%
	Dust	-	-	30%	28%	-
	Other	10%	10%	10%	10%	10%
Hebei[c]	Traffic	-	18%–55%	18%–55%	18%–55%	18%–55%
	Industry	15%–30%	15%–30%	15%–30%	15%–30%	15%–30%
	Dust	-	-	11%–29%	11%–29%	-
	Other	10%	10%	10%	10%	10%

[a] The emission reduction ratio for other sources refers to the pollutant reduction generated by the recommended measures.
[b] There were no control measures implemented for the traffic sources in Tianjin.
[c] The levels of alerts issued in the cities of Hebei province varies (as shown in Fig. 1), and the reduction ratios only considered the cities with alerts issued.

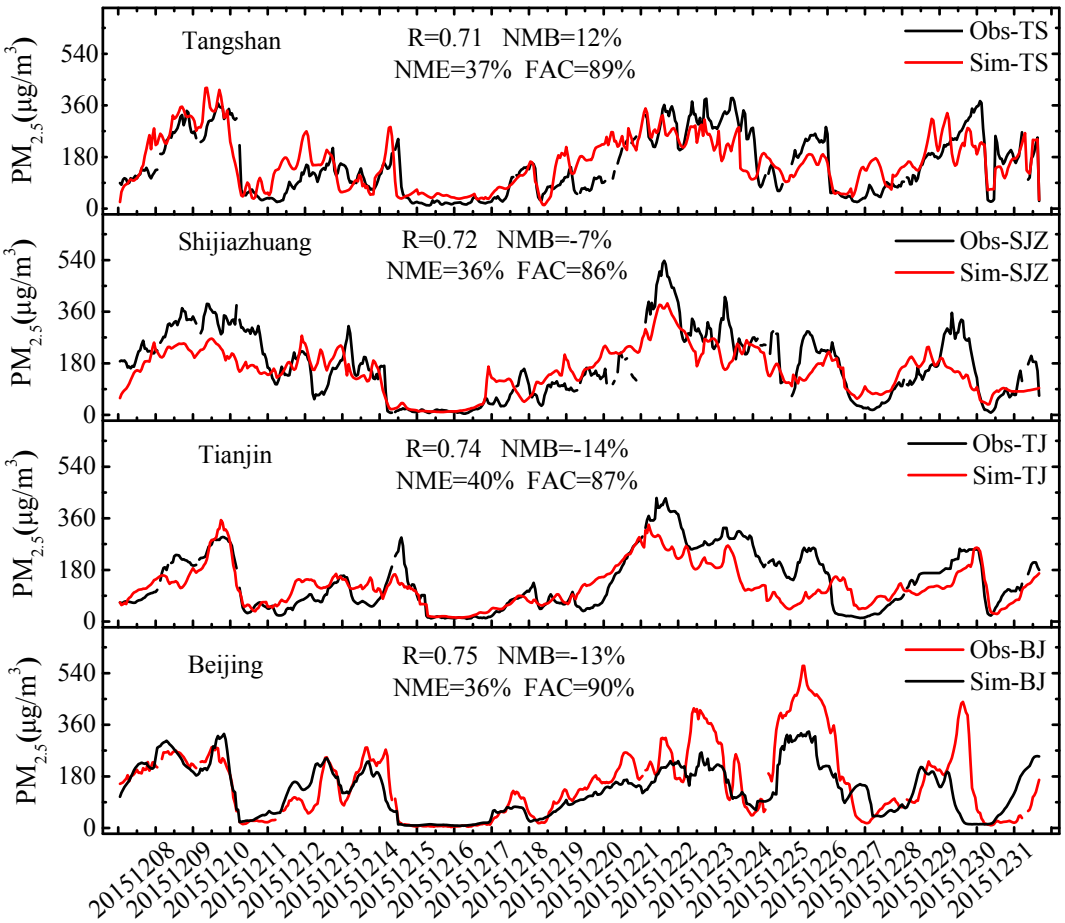

Fig. 3. Comparisons of the simulated and observed $PM_{2.5}$ concentrations for the period of December 7 to 31, 2015 for the sub-areas of BJ, TJ, SJZ and TS.

RESULTS AND DISCUSSION

Meteorological Conditions and $PM_{2.5}$ Evolution Characteristics in December 2015

It is evident from the previous studies that $PM_{2.5}$ concentration is influenced by meteorological conditions, and the MLH is considered to be an important factor causing the variance of $PM_{2.5}$ concentrations (Yang *et al.*, 2015a). Fig. 4 shows the daily $PM_{2.5}$ concentrations and MLH in Beijing in Decembers of 2013, 2014 and 2015. The MLH shows a generally negative correlation with the $PM_{2.5}$ concentrations, and higher $PM_{2.5}$ load near the ground surface was always coupled with a much-lower-than 1000 m MLH for Beijing (Schafer *et al.*, 2009). The horizontal breakpoint lines in Fig. 4 represent a $PM_{2.5}$ concentration of 150 μg m^{-3}, which is the threshold between light pollution and heavy pollution according to the China's National Ambient Air Quality Standard (CNAAQA); they also represent a MLH height of 1000m. Although the total emissions have continued to decline over the past years due to the implementation of the National Total Emission Control Program (NTECP), heavy air pollutions occurred more frequently in December 2015 as compared to Decembers of 2013 and 2014 (Xue *et al.*, 2013). The distribution probability of MLH being below 1000m in Decembers of 2013, 2014 and 2015 were 32.3%, 9.7%, and 48.4%, respectively, indicating that December 2015 had a superior atmospheric stability and the meteorological conditions were thus not favorable for air pollutant diffusion and movement. The meteorological conditions were possibly caused by the strong El Nino effect occurred in the winter of 2015 (Chang *et al.*, 2016; Feng *et al.*, 2016; Wie and Moon, 2016).

Fig. 5 shows the monitored meteorological parameters in Beijing in December 2015, including temperature, air pressure, humidity, and visibility. The bottom graph in Fig. 5 presents the temporal variation and evolution of hourly $PM_{2.5}$ concentrations in the urban area of Beijing. The red horizontal breakpoint line in the bottom graph represents a $PM_{2.5}$ concentration of 150 μg m^{-3}. It is obvious that there were five peak $PM_{2.5}$ concentration sections as labelled in the bottom graph of Fig. 5, and they represent five $PM_{2.5}$ pollution episodes occurred during the 30-day stretch of December 2015. Each heavy pollution episode lasted for different number of days. The highest $PM_{2.5}$ concentration occurred in the fourth episode with a transient concentration of 567 μg m^{-3}. The first red alerts were issued for the first episode, and the second red alert was issued for the third episode, since both episodes lasted for more than 72 hours, while the durations of episodes 2, 4 and 5 were all less than 72 hours.

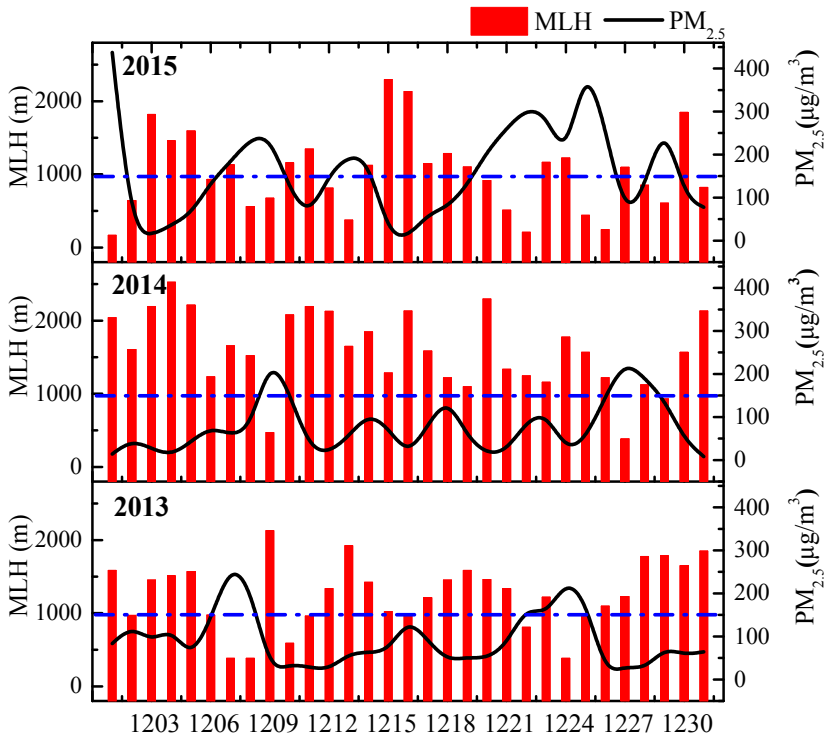

Fig. 4. Daily $PM_{2.5}$ concentrations and MLH in Beijing in Decembers of 2013, 2014 and 2015.

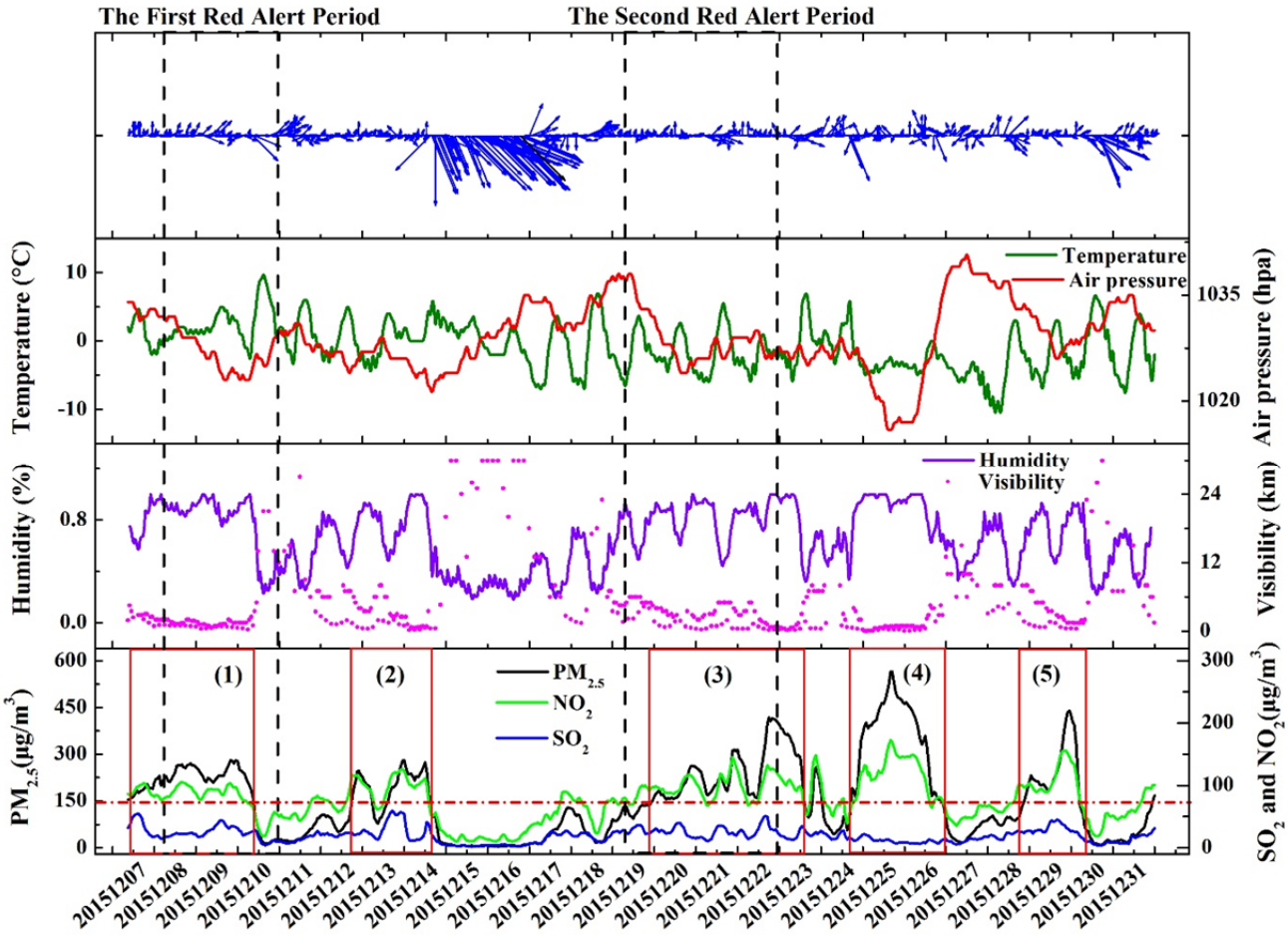

Fig. 5. Hourly $PM_{2.5}$ concentration and meteorological parameters in Beijing in December 2015.

The data in Fig. 5 also demonstrate that $PM_{2.5}$ concentrations in the urban areas of Beijing were negatively correlated with the wind speeds and air pressure, but positively correlated with the relative humidity. Wind can enhance the dispersion of air pollutants out of the region whereas high air pressure constrains the air pollutants in Beijing's airshed. Humidity is associated with the hygroscopicity and scattering of particles (Zhang *et al*., 2015a), which makes the precursors of $PM_{2.5}$ have the tendency to form $PM_{2.5}$ through complex chemical reactions. During the heavy pollution periods in December 2015, south wind with a speed lower than 2 m s^{-1} was dominant and carried the air pollutants (Feng *et al*., 2014a) generated from heavily industrialized Hebei province to Beijing; at the same time, the regional air pressure in Beijing continued to drop and the atmospheric conditions were very stable and stagnant so that the pollutant diffusion and movement in both vertical and horizontal directions were significantly restricted. In addition, high humidity facilitated the hygroscopic growth of aerosols which leads to the increased aerosol mass concentrations and thus low-visibility of air (when the humidity is greater than 80%, the aerosol particulate scattering coefficient is nearly 2 times of that in dry conditions (Yang *et al*., 2015a)).

In other periods of December 2015, the strong northwest winds prevailed so that the meteorological conditions were much improved with increased regional air pressure and decreased humidity. The strong winds also accelerated the horizontal dispersion and vertical diffusion of air pollutants, pushing $PM_{2.5}$ to its downwind directions and thus removing them from Beijing's airshed.

$PM_{2.5}$ Concentration Trend during 2 Red Alert Periods

With the hourly $PM_{2.5}$ concentrations collected from all the monitoring stations in BTH region, the Kriging interpolation method built into Geographic Information System (GIS) was used as a spatial interpolation technique to analyze the entire heavy pollutions in December 2015, particularly for the two red alert periods in the BTH region. The semi-variogram method was used to quantity the spatial variation of regionalized variables (Yang *et al*., 2008).

The First Red Alert Period

Fig. 6 presents four graphs of the regional air pressure patterns during the first red alert period at 8:00AM for 4 consecutive days from December 7 to 10. It is observed that the BTH study region was under control of a high-pressure center and system on December 7, a sparse-isobar pressure system on December 8, a low-pressure center and system on December 9, and an intensive-isobar pressure system on December 10, respectively. During the first red alert period, the emergency control measures were implement on December 8, and the BTH region was then under control by a sparse-isobar pressure system with widely spaced isobars, and the horizontal composition and movement of the atmosphere were relatively stagnant. These conditions made the air pollutants be easily trapped and accumulated in Beijing's airshed. On December 9, a low-pressure center was formed around the BTH region, and the air masses (containing air pollutants) were driven into the BTH region from the surrounding provinces; as a result, $PM_{2.5}$ concentrations in Beijing increased dramatically. The $PM_{2.5}$ concentrations have remained high till December 10 when an intensive-isobar pressure system moved into the region and brought high-speed winds to help push the air pollutants out of the region.

Fig. 7 shows the evolution of $PM_{2.5}$ concentration in the BTH region over the first alert period. At 8:00AM on December 7, the entire BTH region had a relatively fair air quality with the $PM_{2.5}$ concentration being lower than 150 μg m^{-3}. 24 hours later at 8:00AM on December 7, $PM_{2.5}$ concentrations have increased dramatically to a level of over 250 μg m^{-3} in the southern part of the BTH region, and heavy pollutions were formed in the southern part and started to spread and moved towards the northern parts of the region. The air movement was obstructed by the Yanshan and Taihang Mountains in the west and north of the BTH region, and as a result, the pollutants stopped moving forward and got accumulated in Beijing's airshed. This explains why Beijing and most area of other BTH region have remained under heavy air pollutions on December 8 and 9. On December 10, an intensive-isobar pressure system brought high-speed winds to disperse the air pollutants out of the region, and the severity of pollution was significantly reduced so that the first red alert was cancelled on that day. It is obvious that the heavy pollution during the first red alert period was severed not only by transboundary emissions from outside sources but also by unfavorable meteorological conditions. It should be pointed out that, the heavy pollution has been formed in Beijing since December 7 while the first red alert was issued till December 8, and therefore the red alert was issued too late considering a general requirement of 24-hour ahead prior to the occurrence of a heavy pollution. Furthermore, the late red alert has delayed the actions of implementing the emergency control measures so that their effects could be negatively jeopardized.

The Second Red Alert Period

It was observed that the regional air pressure systems over the BTH region during the second red alert period were similar to that in the first red alert period, and this makes the $PM_{2.5}$ pollution evolve similarly as well.

Fig. 8 shows the evolution of $PM_{2.5}$ concentrations in the BTH region over the second red alert period. On December 18, there was no heavy pollution formed in the BTH region. From December 19, the pollutants began to gradually accumulate in Beijing and the middle parts of the BTH region and tended to spread to the surrounding areas. One day later on December 20, Beijing and its surrounding areas experienced heavy air pollutions. This situation continued till December 23 when the strong northwest winds blew through the region. It is obvious that the heavy pollution occurred in Beijing during the second red alert period was mainly caused by local emissions and accumulation of pollutants in the study region. The second red alert was issued at 7:00AM on December 19 and was regarded as a imely issuing in comparison to the issuing time of the first red alert. The timely action could possibly enhance the

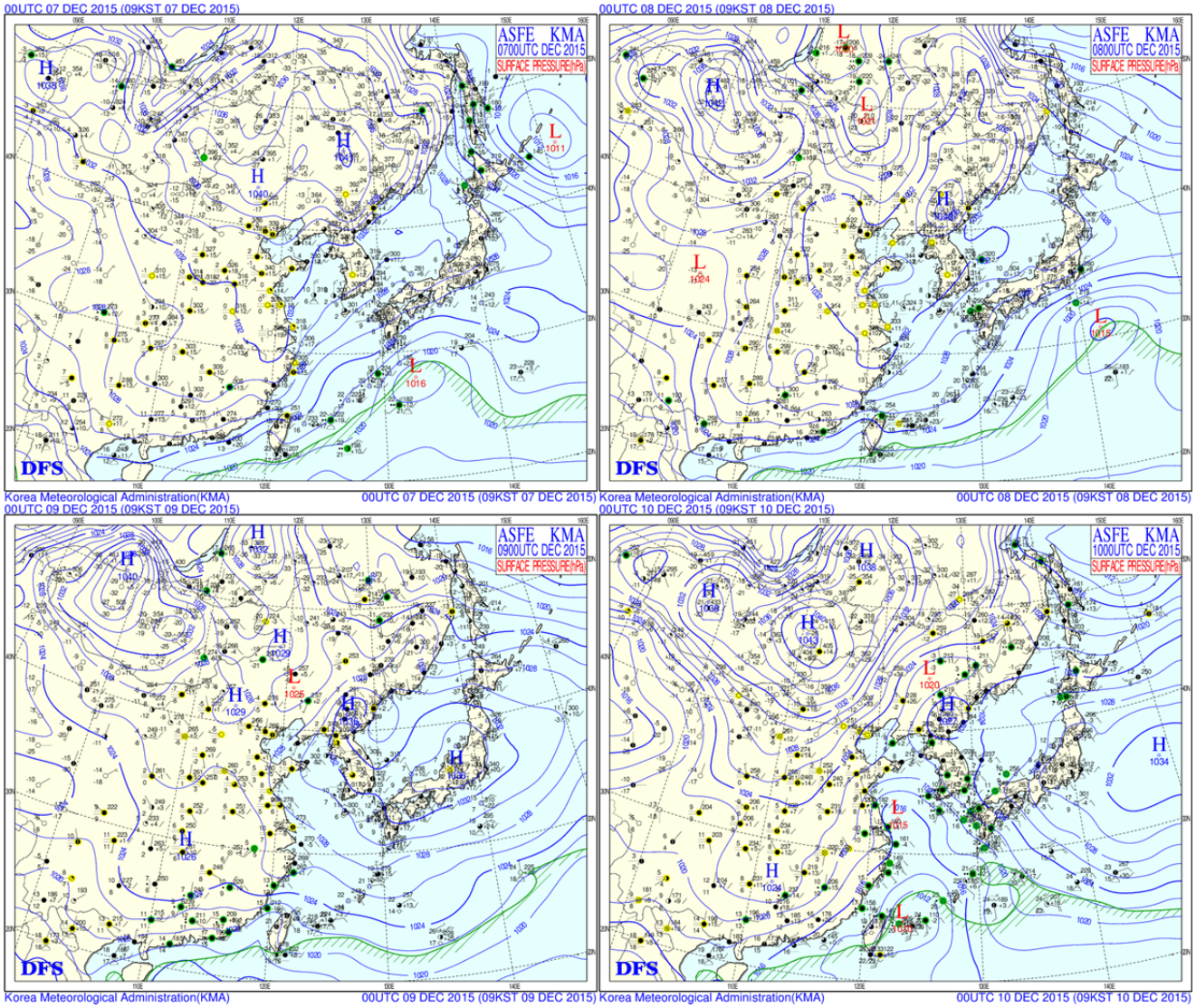

Fig. 6. Air pressure patterns over the BTH region at 8:00AM from December 7 to 10 in 2015 (Note: blue lines represent isobars; air pressure unit: hpa; H and L represent high and low pressure centers).

effects of implementing emergency control measures on air pollution control (Liu *et al*., 2013).

$PM_{2.5}$ Source Apportionment and Contribution Analysis

Fig. 9 compares the percentages of $PM_{2.5}$ contributions from different sub-areas and different emission categories to the urban area of Beijing among no-heavy-pollution period, the first red alert period, and the second red alert period in December 2015. The $PM_{2.5}$ concentrations were obtained by the WRF-CAMx modeling system.

Fig. 9 shows that, in the no-heavy-pollution period, $PM_{2.5}$ in Beijing originated mainly from local emissions with a total percentage of 76.0% (57.7% from BJ-U and 18.3% from BJ-R). This was due to relatively stable meteorological conditions occurred during these no-heavy-pollution days in December 2015 (such as low-speed wind and stagnant weather). The contribution percentages from surrounding sub-areas were pretty low, and main external sources including BD, CD and TS contributed only 3.4%, 2.9%, 2.9%, respectively, to the total. Among various emission categories in the BTH region, the sequence of contribution percentage is traffic (27.9%), coal (21.4%), dust (16.3%), industry (14.9%), and others (13.1%). For the BJ-U area, traffic (19.7%) and coal (15.0%) were the main contributors among all the local emission categories. This is not surprising at all considering the facts that December is the heating season in Beijing for more coal consumption and the number of vehicles on road and thus traffic volume in Beijing have increased significantly in the past two decades. In addition, the coal and vehicles were the main sources for emitting SO_2 and NO_2 into the atmosphere as well. As shown in Fig. 5, in December 2015, the observed SO_2 concentration (with an hourly mean concentration of 19.7 μg m^{-3}) was much lower than the observed NO_2 concentration (with an hourly mean concentration of 78.1 μg m^{-3}) in Beijing. The emitted SO_2 could be transformed and converted into sulfate by a liquid-phase oxidation process (Li *et al*., 2015a), which might be further facilitated by the high humidity in

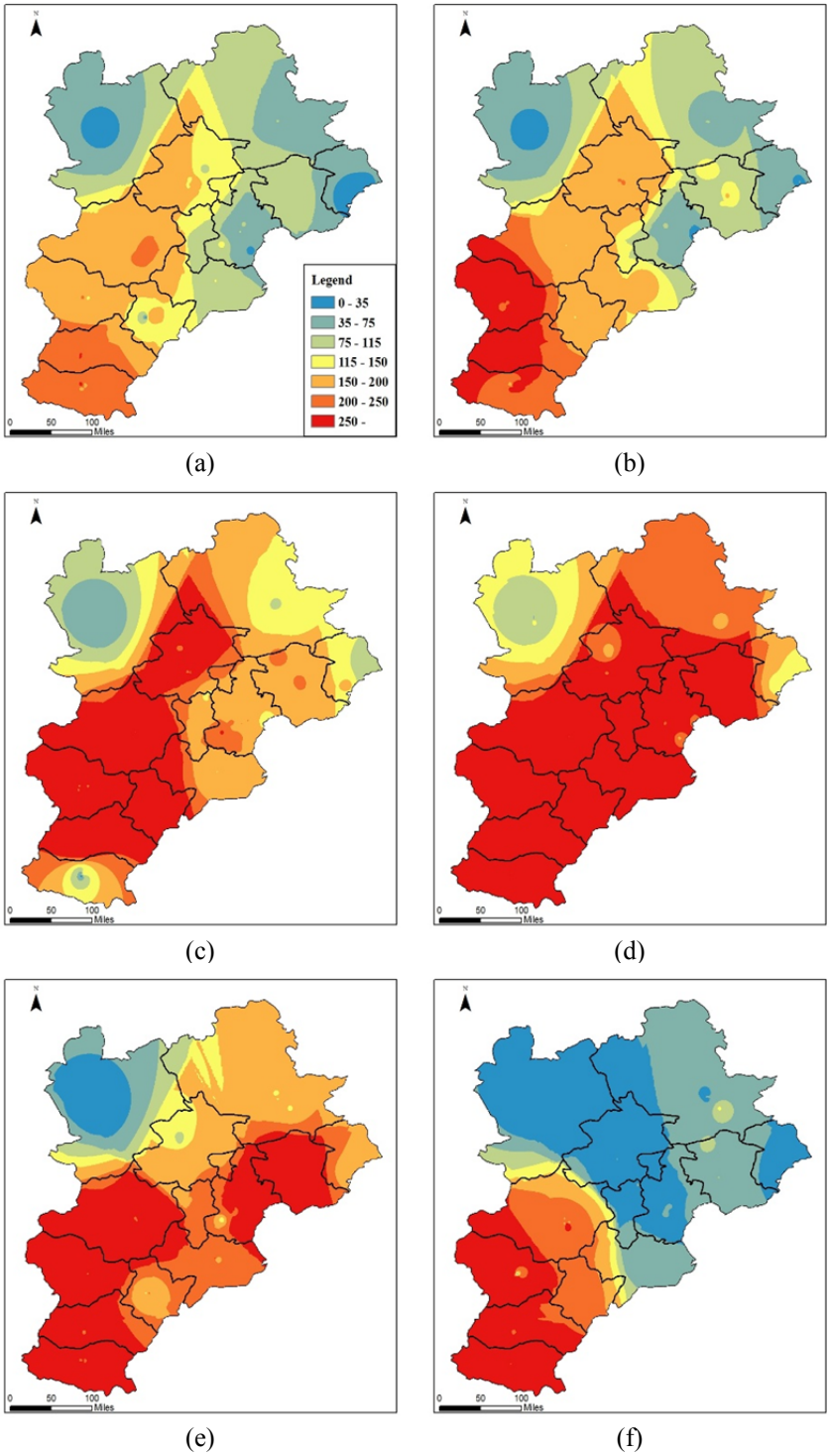

Fig. 7. Evolution of $PM_{2.5}$ concentration (unit: μg m^{-3}) in BTH region over the first red alert period: (a) 8:00 AM on December 7, (b) 8:00 PM on December 7, (c) 8:00AM on December 8, (d) 8:00 AM on December 9, (e) 8:00 AM on December 10, (f) 8:00 PM on December 10.

December 2015; instead, the photochemical conversion of NO_x to nitrate needs sunlight and high temperature, and the weather conditions in December 2015 did not favor the conversion process (Zhao *et al.*, 2013).

As shown in Fig. 9, in the first red alert period, the contribution percentage from local emission sources in Beijing decreased to 64.8% (including a percentage of 45.3% from BJ-U and a percentage of 19.5% from BJ-R) in comparison to 76% in no-heavy-pollution periods. This indicates increased transboundary contributions of pollutants from surrounding areas. The modeling results show that the contribution percentages from sub-areas or cities in the

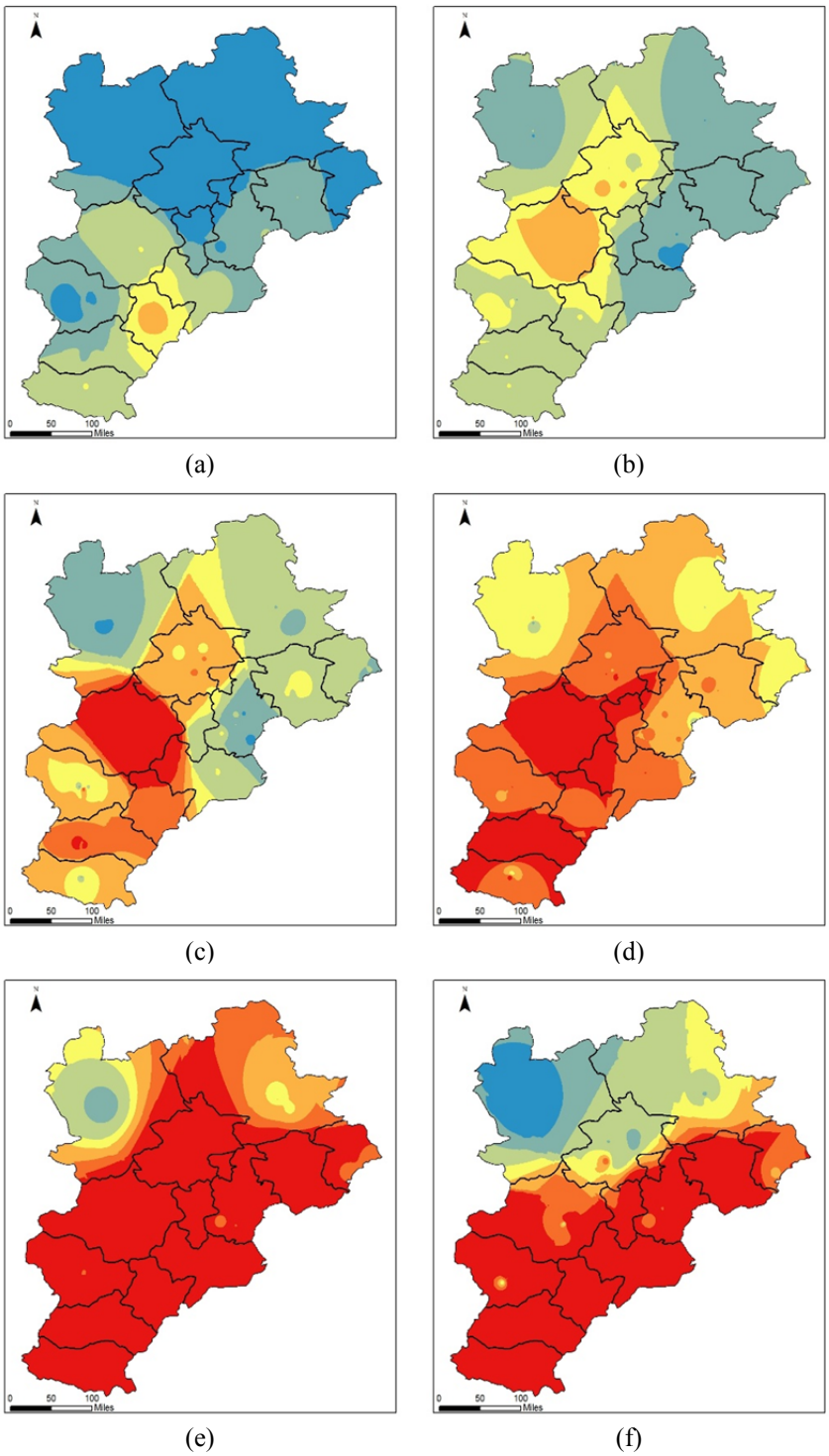

Fig. 8. Evolution of $PM_{2.5}$ concentration (unit: μg m^{-3}) in BTH region over the second red alert period: (a) 4:00 PM on December 18, (b) 4:00 PM on December 19, (c) 4:00 AM on December 20, (d) 6:00 PM on December 20, (e) 10:00 AM on December 22, (f) 4:00 PM on December 23. *The legend in Fig. 8 is same as Fig. 7.

southern part of the region increased significantly. For example, the contribution percentage from BD was increased to 9.3% which was doubled more than that in no-heavy-pollution periods; similar observations can be found for LF (3.4%) and SJZ (2.0%). However, the contribution percentages from the northern sub-areas remained nearly unchanged. Among all the 5 emission categories, the coal became the largest source with a contribution percentage of 31.2% in the first red alert period, while the contribution percentages from the traffic, industry, and construction dust were 22.6%, 16.8%, and 10.4%, respectively. During the first red alert period, the implemented emergency control

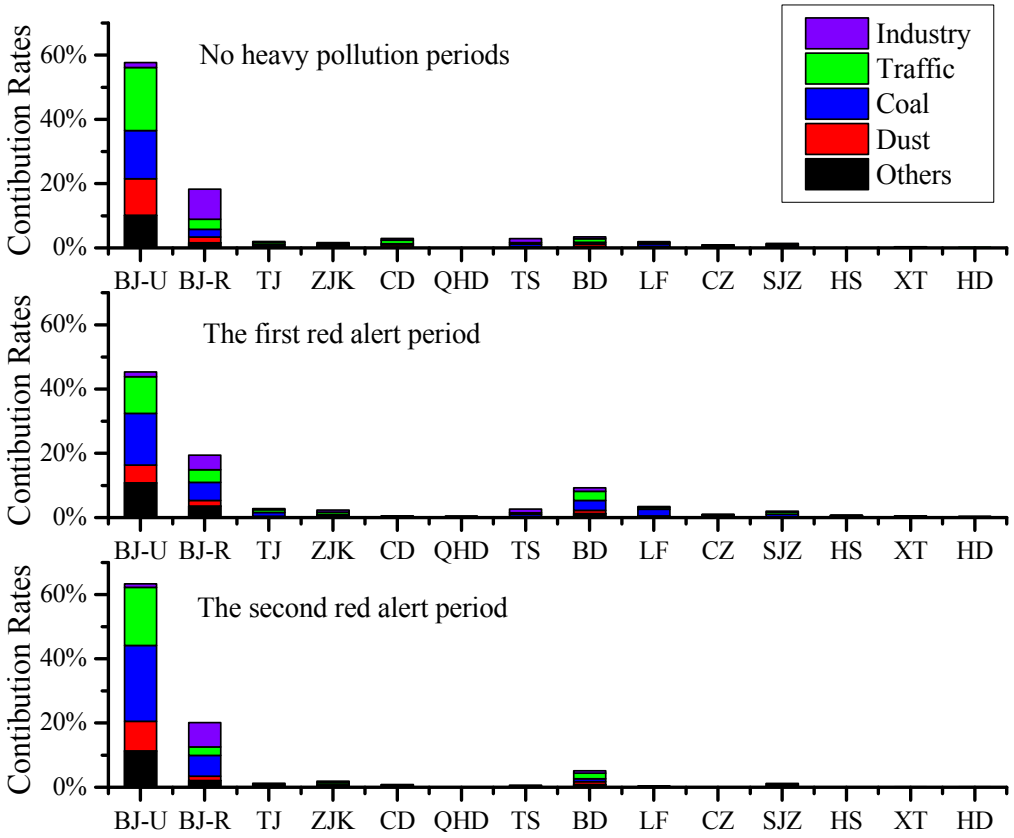

Fig. 9. The percentages of $PM_{2.5}$ contributions from different sub-areas and different emission categories to the urban area of Beijing among no-heavy-pollution period, the first red alert period, and the second red alert period in December 2015.

measures consisted mainly of traffic volume reduction, industrial plants shutdown, and construction project suspension, and no actions were taken for reducing the coal combustion and domestic boiler usage, and as a result. In addition, local coal consumption and traffics were top two largest sources contributing percentages of 16.1% and 11.4%, respectively, to the $PM_{2.5}$ concentration in BJ-U among all the sources in the BTH region. It is apparent that the emergency control measures played a vital role in changing the emission contribution percentages among different emission categories during the first red alert period.

During the second red alert period, the contribution percentage from local emission sources in Beijing increased to 83.5% with 63.4% from BJ-U and 20.1% from BJ-R. This indicates the heavy pollution occurred in the second red alert period was mainly caused by local pollutant accumulation. The contribution percentages from transboundary sources in the surrounding sub-areas and cities were generally less than that in no-heavy-pollution periods or the first red alert period, and this was due mainly to the relatively stable meteorological conditions in the second red alert period. As for the emission categories, the coal (32.4%) was the highest contributor in the second red alert period, followed by the traffic (24.7%), others (14.7%), dust (12.4%) and industry (10.8%). Similarly, the coal consumption (23.6%) and traffics (18.1%) were top two contributors to the $PM_{2.5}$ pollutions in BJ-U with a percentage of 23.6% and 18.1%, respectively. The ranking of contribution percentages of different emission categories could help the governmental authorities to make and select appropriate emergency control measure when facing heavy pollution conditions.

Impact Analysis of the Emergency Control Measures on $PM_{2.5}$ Concentration

In this study, four simulation scenarios (i.e., BASE, NC, NBC, and NHTC) were designed and simulated through the WRF-CAMx modeling system for assessing the effects of the emergency control measures on $PM_{2.5}$ concentration changes.

Overall Effects Analysis

Fig. 10 shows the simulated mean $PM_{2.5}$ concentrations in BJ-U under four designed simulation scenarios for the first and second red alert periods, respectively. The simulation results were used to examine the effects of implementing emergency control measures on $PM_{2.5}$ concentrations.

As shown in Fig. 10, during the first red alert period, the mean $PM_{2.5}$ concentrations of BASE, NC, NBC and NHTC scenarios were 239.5 μg m^{-3}, 289.0 μg m^{-3}, 261.5 μg m^{-3} and 265.5 μg m^{-3}, respectively. The observations from the simulation results entail: (1) the mean $PM_{2.5}$ concentration under BASE scenario was the lowest one among all four scenario, implying that the emergency control measures implemented in the BTH region during the first red alert period were effective in reducing the $PM_{2.5}$ concentration

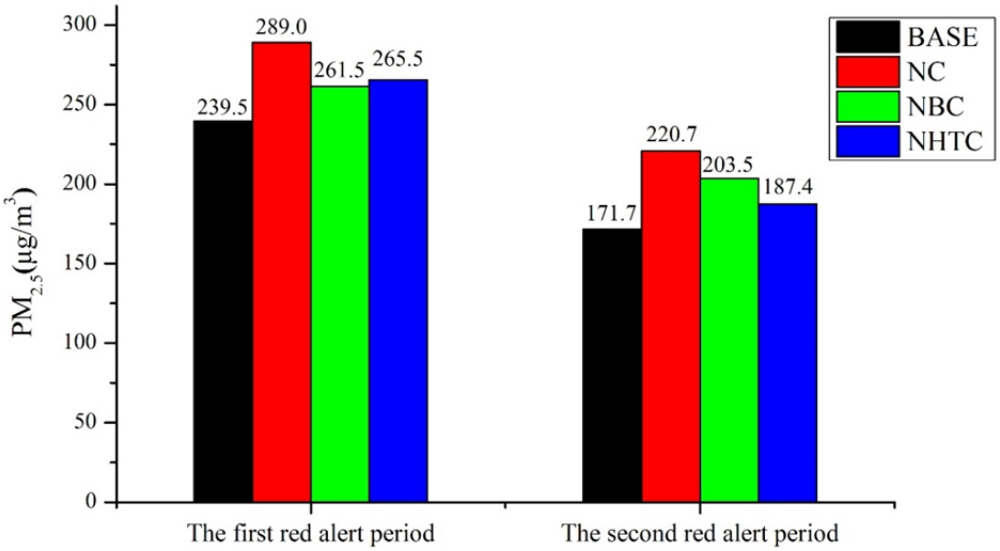

Fig. 10. The simulated mean $PM_{2.5}$ concentrations in BJ-U under four designed simulation scenarios for both red alert periods.

in the urban area of Beijing; (2) the NC scenario refers to the situation that no any emergency control measures were implemented in the study region during the first red alert period. Under this scenario, the simulated mean $PM_{2.5}$ concentration in BJ-U was the highest one, which indicates again the emergency control measures have positive effects in mitigating the $PM_{2.5}$ pollution; (3) the NBC and NHTC scenarios refer to the situations that the emergency control measures were implemented only in the areas outside Beijing or in the areas only inside Beijing. The simulated mean $PM_{2.5}$ concentrations under the NHTC scenario was slightly higher that under the NBC scenario, but both were higher than the BASE scenario and lower than the NC scenario. It is indicated that not only the emergency control measures were generally effective, but also the areas where they were implemented played a vital role in $PM_{2.5}$ pollution control.

During the second red alert period, the mean $PM_{2.5}$ concentration of BASE, NC, NBC and NHTC scenarios were 171.7 μg m^{-3}, 220.7 μg m^{-3}, 203.5 μg m^{-3} and 187.4 μg m^{-3}, respectively. Similar observations could be obtained. For example, the mean $PM_{2.5}$ concentration under BASE scenario was lowest and that under NC scenario were highest, which means implementing the emergency control measure had positive effects in reducing $PM_{2.5}$ pollution in Beijing. In the second red alert period, the mean $PM_{2.5}$ concentration under NHTC scenario is a little lower than that under NBC scenario, which means implementing emergency control measures in the areas of Beijing had better effects in $PM_{2.5}$ pollution control.

According to the simulated mean $PM_{2.5}$ concentrations under BASE and NC scenarios, the reduction ratios of $PM_{2.5}$ concentration in BJ-U can be calculated. The calculated reduction ratios for the first and second red alert periods were 17.1% and 22.2%, respectively. It is indicated that, although same emergency control measures were implemented during two red alert periods, their effects on $PM_{2.5}$ pollution control in the first red alert period was obviously lower than that in the second red alert period. The reasons behind this difference might remain unknown exactly, however, one possible explanation is that the implementation of emergency control measures was delayed almost 2 days due the late issuing of the first red alert. If the first red alert could be issued earlier, a large portion of the pollutants emitted from various sources in the study region could be reduced before the heavy pollution was formed in the region, and this would lead to a higher $PM_{2.5}$ concentration reduction ratio. It is suggested that the 24-hour rule for issuing the red alert should be reinforced by the government in order to maximizing the effects of the emergency control measures.

Effect Analysis for Individual Emergency Control Measure

The effects of individual emergency control measure on $PM_{2.5}$ reduction were also examined through the WRF-CAMx simulation modeling system. The emergency control measures were ranked in terms of their effectiveness in $PM_{2.5}$ pollution control.

Fig. 11 shows the reduced $PM_{2.5}$ concentrations from the implementation of individual emergency control measures in BJ-U during two red alert periods. The individual emergency control measure under examination consists of control actions taken for four different emission categories (i.e., industry, traffic, dust and the others). During the first red alert period, the average reduced $PM_{2.5}$ concentrations in BJ-U from implementing four individual control measure in the BTH region were 14.1 μg m^{-3} for industry, 21.5 μg m^{-3} for traffic, 6.6 μg m^{-3} for dust, and 3.9 μg m^{-3} for the others, respectively. It is obvious that the reduction from the traffic volume control measures (such as the odd-and-even license plate rule) was highest among all four emission control categories. In terms of the reduction contributions from all the emission sub-areas, the largest $PM_{2.5}$ concentration reduction in BJ-U came from the control

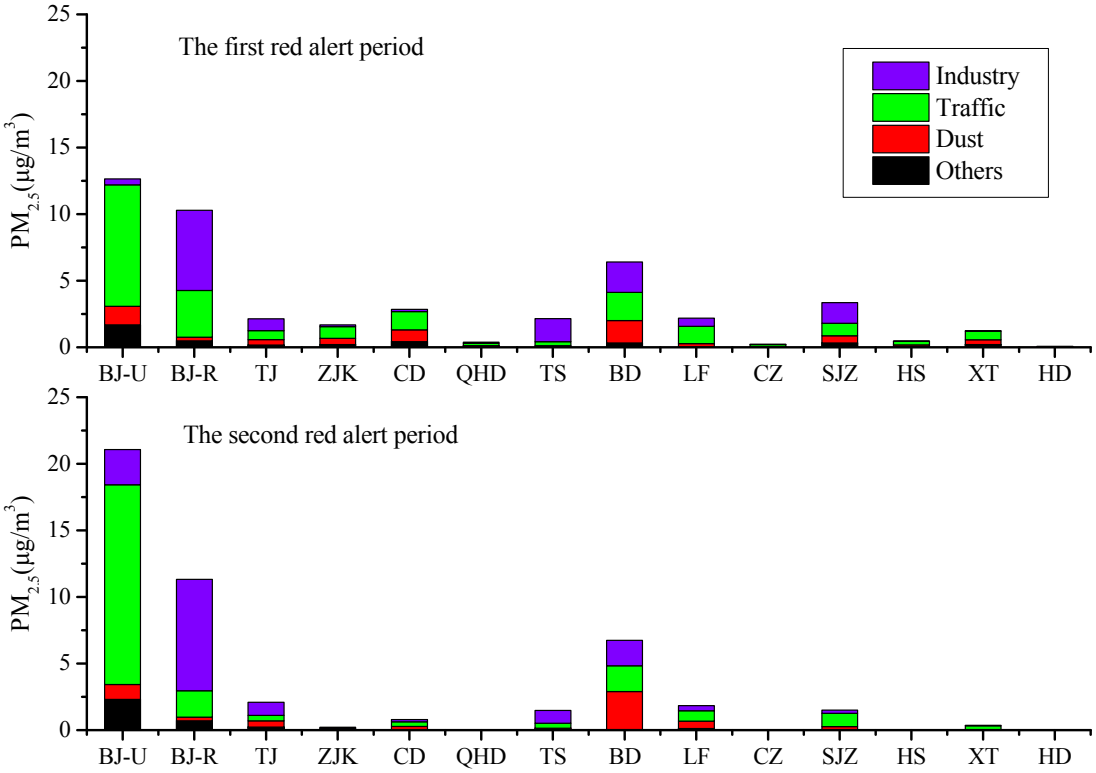

Fig. 11. The $PM_{2.5}$ concentration reductions from the implementation of individual emergency control measure in BJ-U during two red alert periods.

measures implemented in the sub-areas outside Beijing with an amount of 26.0 μg m^{-3} in the first red alert period. It is obvious that the implementation of emergency control measures in the southern part of the study region played a critical role in improving the air quality in Beijing.

During the second red alert period, the average reduced $PM_{2.5}$ concentrations in BJ-U from implementing four individual control measure in the BTH region were 15.7 μg m^{-3} for industry category, 22.3 μg m^{-3} for traffic category, 6.0 μg m^{-3} for dust category, and 3.4 μg m^{-3} for other categories. Again the reduction from implementing traffic volume control measures was highest among all four emission control categories.

The effects of implementing control measures on four emission categories in the sub-areas of BJ-U and BJ-R were examined due to their significant differences in industrial settings and traffic volume. During the second red alert period, the average reduced $PM_{2.5}$ concentrations in BJ-U from implementing four individual control measure in the urban area of Beijing were 2.7 μg m^{-3} for industrial category, 15.0 μg m^{-3} for traffic category, 2.3 μg m^{-3} for dust category, and 1.1 μg m^{-3} for other categories. In contrast, the average reduced $PM_{2.5}$ concentrations in BJ-U from implementing four individual control measure in the rural area of Beijing were 8.4 μg m^{-3} for industrial category, 2.0 μg m^{-3} for traffic category, 0.3 μg m^{-3} for dust category, and 0.7 μg m^{-3} for other categories. It is apparent that implementing control measures for traffic category in the urban area of Beijing was most effective in $PM_{2.5}$ concentration reduction while implementing control measures for industrial category in the rural area of Beijing was most effective. This is in accordance with the functions for different sub-areas of Beijing municipality, which should be put into consideration when implementing emergency control measures for alleviating or preventing the occurrence of heavy air pollutions.

CONCLUSIONS

In December 2015, 2 red alerts were issued by Beijing municipal government and various emergency control measures were also implemented in the BTH region to alleviate the negative effects of severe air pollutions occurred in Beijing. In order to assess the effects of these emergency control measures on pollution control in Beijing, in this study, the WRF-CAMx modeling system was implemented over the 2-level-nested grid BTH domain to simulate spatial and temporal variations of the $PM_{2.5}$ concentration in Beijing during 2 red alert periods. The model was verified through 4 statistical approaches, and an acceptable agreement between the simulated and observed concentrations has been achieved. The simulation results show that the heavy pollution in Beijing was formed by transboundary emissions from outside sources in the first red alert period, while the heavy pollution was mainly caused by local emissions and accumulation of pollutants in the second red alert period due to stable atmospheric conditions. Four emission-reduction-control scenarios were then designed and simulated by the modeling system for quantitatively assessing the effects of the emergency control measures on $PM_{2.5}$ concentration

evolution. It is evident from the results that the control measures implemented in Beijing and its surrounding areas during the 2 red alert periods could generally improve the air quality in urban area of Beijing, and the control measures in the categories of traffic volume control and industrial operation suspension were the most effective one among all the individual emergency control measures for both red alert period. It is recommended that joint and collective control efforts in the BTH region be developed for improving environmental performance and achieving better results in the long-term.

ACKNOWLEDGEMENT

This work was supported by the National Natural Science Foundation of China (No. 91544232 & 51638001) and the Ministry of Environmental Protection Special Funds for Scientific Research on Public Causes (No. 201409006). In addition, we greatly appreciated the fund support from Beijing Municipal Commission of Science and Technology (No. D16110900440000 & D161100004416001). The authors are grateful to the anonymous reviewers for their insightful comments.

REFERENCE

Akritidis, D., Zanis, P., Pytharoulis, I. and Karacostas, T. (2014). Near-surface ozone trends over Europe in RegCM3/CAMx simulations for the time period 1996–2006. *Atmos. Environ.* 97: 6–18.

Bi, J.R., Huang, J.P., Hu, Z.Y., Holben, B.N. and Guo, Z.Q. (2014). Investigating the aerosol optical and radiative characteristics of heavy haze episodes in Beijing during January of 2013. *J. Geophys. Res.* 119: 9884–9900.

Chang, L.Y., Xu, J.M., Tie, X.X. and Wu, J.B. (2016). Impact of the 2015 El Nino event on winter air quality in China. *Sci. Rep.* 6: 34275.

Chen, H.S., Li, J., Ge, B.Z., Yang, W.Y., Wang, Z.F., Huang, S., Wang, Y.L., Yan, P.Z., Li, J.J. and Zhu, L.L. (2015a). Modeling study of source contributions and emergency control effects during a severe haze episode over the Beijing-Tianjin-Hebei area. *Sci. China Chem.* 58: 1403–1415.

Chen, T.F., Chang, K.H. and Tsai, C.Y. (2014). Modeling direct and indirect effect of long range transport on atmospheric $PM_{2.5}$ levels. *Atmos. Environ.* 89: 1–9.

Chen, Z., Zhang, J., Zhang, T., Liu, W. and Liu, J. (2015b). Haze observations by simultaneous lidar and WPS in Beijing before and during APEC, 2014. *Sci. China Chem.* 58: 1385–1392.

Cheng, S., Li, L., Chen, D. and Li, J. (2012). A neural network based ensemble approach for improving the accuracy of meteorological fields used for regional air quality modeling. *J. Environ. Manage.* 112: 404–414.

Dong, X.Y., Gao, Y., Fu, J.S., Li, J., Huang, K., Zhuang, G.S. and Zhou, Y. (2013). Probe into gaseous pollution and assessment of air quality benefit under sector dependent emission control strategies over megacities in Yangtze River Delta, China. *Atmos. Environ.* 79: 841–852.

Feng, J., Li, J.P., Zhu, J.L. and Liao, H. (2016). Influences of El Nino modoki event 1994/1995 on aerosol concentrations over southern China. *J. Geophys. Res.* 121: 1637–1651.

Feng, X., Li, Q., Zhu, Y., Wang, J., Liang, H. and Xu, R. (2014a). Formation and dominant factors of haze pollution over Beijing and its peripheral areas in winter. *Atmos. Pollut. Res.* 5: 528–538.

Feng, X., Li, Q. and Zhu, Y.J. (2014b). Bounding the role of domestic heating in haze pollution of Beijing based on satellite and surface observations. 2014 IEEE International Geoscience and Remote Sensing Symposium (IGARSS), Quebec City, Canada, pp. 4772–4775.

Guo, S., Hu, M., Zamora, M.L., Peng, J., Shang, D., Zheng, J., Du, Z., Wu, Z., Shao, M., Zeng, L., Molina, M.J. and Zhang, R. (2014). Elucidating severe urban haze formation in China. *Proc. Natl. Acad. Sci. U.S.A.* 111: 17373–17378.

He, X.W., Xue, Y., Guang, J., Shi, Y.L., Xu, H., Cai, J.M., Mei, L.L. and Li, C. (2014). The analysis of the haze event in the North China Plain in 2013. 2014 IEEE International Geoscience and Remote Sensing Symposium (IGARSS), Quebec City, Canada, pp. 5002–5005.

Huang, K., Zhang, X. and Lin, Y. (2015). The "APEC Blue" phenomenon: Regional emission control effects observed from space. *Atmos. Res.* 164–165: 65–75.

Jiang, C., Wang, H., Zhao, T., Li, T. and Che, H. (2015). Modeling study of $PM_{2.5}$ pollutant transport across cities in China's Jing-Jin-Ji region during a severe haze episode in December 2013. *Atmos. Chem. Phys.* 15: 5803–5814.

Koo, B., Kumar, N., Knipping, E., Nopmongcol, U., Sakulyanontvittaya, T., Odman, M.T., Russell, A.G. and Yarwood, G. (2015). Chemical transport model consistency in simulating regulatory outcomes and the relationship to model performance. *Atmos. Environ.* 116: 159–171.

Lang, J., Cheng, S., Zhou, Y., Zhao, B., Wang, H. and Zhang, S. (2013a). Energy and environmental implications of hybrid and electric vehicles in China. *Energies* 6: 2663–2685.

Lang, J.L., Cheng, S.Y., Li, J.B., Chen, D.S., Zhou, Y., Wei, X., Han, L.H. and Wang, H.Y. (2013b). A monitoring and modeling study to investigate regional transport and characteristics of $PM_{2.5}$ pollution. *Aerosol Air Qual. Res.* 13: 943–956.

Li, L., An, J.Y., Zhou, M., Yan, R.S., Huang, C., Lu, Q., Lin, L., Wang, Y.J., Tao, S.K., Qiao, L.P., Zhu, S.H. and Chen, C.H. (2015a). Source apportionment of fine particles and its chemical components over the Yangtze River Delta, China during a heavy haze pollution episode. *Atmos. Environ.* 123: 415–429.

Li, X., Zhang, Q., Zhang, Y., Zheng, B., Wang, K., Chen, Y., Wallington, T.J., Han, W.J., Shen, W., Zhang, X.Y. and He, K.B. (2015b). Source contributions of urban $PM_{2.5}$ in the Beijing-Tianjin-Hebei region: Changes between 2006 and 2013 and relative impacts of emissions and meteorology. *Atmos. Environ.* 123: 229–239.

Li, Y., Lau, A.K.H., Fung, J.C.H., Ma, H. and Tse, Y.Y. (2013). Systematic evaluation of ozone control policies using an ozone source apportionment method. *Atmos.*

Environ. 76: 136–146.

Liu, H., Wang, X., Zhang, J., He, K., Wu, Y. and Xu, J. (2013). Emission controls and changes in air quality in guangzhou during the asian Games. *Atmos. Environ.* 76: 81–93.

Megaritis, A.G., Fountoukis, C. and Pandis, S.N. (2014). Sensitivity of fine PM levels in Europe to emissions changes. In *Air Pollution Modeling and its Application XXII*. Steyn, D., Builtjes, P. and Timmermans, R. (Eds.), NATO Science for Peace and Security Series C: Environmental Security. Springer, Dordrecht, pp. 333–338.

Pirovano, G., Colombi, C., Balzarini, A., Riva, G.M., Gianelle, V. and Lonati, G. (2015). $PM_{2.5}$ source apportionment in Lombardy (Italy): Comparison of receptor and chemistry-transport modelling results. *Atmos. Environ.* 106: 56–70.

Qu, Y., An, J.L., Li, J., Chen, Y., Li, Y., Liu, X.G. and Hu, M. (2014). Effects of NO_x and VOCs from five emission sources on summer surface O_3 over the Beijing-Tianjin-Hebei region. *Adv. Atmos. Sci.* 31: 787–800.

Schafer, K., Wang, Y.S., Munkel, C., Emeis, S., Xin, J.Y., Tang, G.Q., Norra, S., Schleicher, N., Vogt, J. and Suppan, P. (2009). Evaluation of continuous ceilometer-based mixing layer heights and correlations with $PM_{2.5}$ concentrations in Beijing. Proc. SPIE 7475, Remote Sensing of Clouds and the Atmosphere XIV, Berlin, Germany.

Shen, J., Wang, X., Li, J., Li, Y. and Zhang, Y. (2011). Evaluation and intercomparison of ozone simulations by Models-3/CMAQ and CAMx over the Pearl River Delta. *Sci. China Chem.* 54: 1789–1800.

Wang, B., Qiu, T. and Chen, B.Z. (2014a). Photochemical process modeling and analysis of ozone generation. *Chin. J Chem. Eng.* 22: 721–729.

Wang, L.L., Liu, Z.R., Sun, Y., Ji, D.S. and Wang, Y.S. (2015a). Long-range transport and regional sources of $PM_{2.5}$ in Beijing based on long-term observations from 2005 to 2010. *Atmos. Res.* 157: 37–48.

Wang, L.T., Wei, Z., Wei, W., Fu, J.S., Meng, C.C. and Ma, S.M. (2015b). Source apportionment of $PM_{2.5}$ in top polluted cities in Hebei, China using the CMAQ model. *Atmos. Environ.* 122: 723–736.

Wang, S., Gao, J., Zhang, Y., Zhang, J., Cha, F., Wang, T., Ren, C. and Wang, W. (2014b). Impact of emission control on regional air quality: An observational study of air pollutants before, during and after the Beijing Olympic Games. *J. Environ. Sci.* 26: 175–180.

Wang, S.X., Zhao, M., Xing, J., Wu, Y., Zhou, Y., Lei, Y., He, K.B., Fu, L.X. and Hao, J.M. (2010). Quantifying the air pollutants emission reduction during the 2008 Olympic Games in Beijing. *Environ. Sci. Technol.* 44: 2490–2496.

Wang, X., Westerdahl, D., Chen, L.C., Wu, Y., Hao, J., Pan, X., Guo, X. and Zhang, K.M. (2009). Evaluating the air quality impacts of the 2008 Beijing Olympic Games: On-road emission factors and black carbon profiles. *Atmos. Environ.* 43: 4535–4543.

Wei, Z., Wang, L.T., Chen, M.Z. and Zheng, Y. (2014). The 2013 severe haze over the southern Hebei, China: $PM_{2.5}$ composition and source apportionment. *Atmos. Pollut. Res.* 5: 759–768.

Wie, J. and Moon, B.K. (2016). Seasonal relationship between meteorological conditions and surface ozone in Korea based on an offline chemistry-climate model. *Atmos. Pollut. Res.* 7: 385–392.

Wu, D., Fung, J.C.H., Yao, T. and Lau, A.K.H. (2013). A study of control policy in the Pearl River Delta region by using the particulate matter source apportionment method. *Atmos. Environ.* 76: 147–161.

Xing, J., Zhang, Y., Wang, S., Liu, X., Cheng, S., Zhang, Q., Chen, Y., Streets, D.G., Jang, C., Hao, J. and Wang, W. (2011). Modeling study on the air quality impacts from emission reductions and atypical meteorological conditions during the 2008 Beijing Olympics. *Atmos. Environ.* 45: 1786–1798.

Xue, W., Wang, J., Niu, H., Yang, J., Han, B., Lei, Y., Chen, H. and Jiang, C. (2013). Assessment of air quality improvement effect under the national total emission control program during the Twelfth National Five-Year Plan in China. *Atmos. Environ.* 68: 74–81.

Yan, R.C., Yu, S.C., Zhang, Q.Y., Li, P.F., Wang, S., Chen, B.X. and Liu, W.P. (2015). A heavy haze episode in Beijing in February of 2014: Characteristics, origins and implications. *Atmos. Pollut. Res.* 6: 867–876.

Yang, J., Huang, Z.C., Chen, T.B., Lei, M., Zheng, Y.M., Zheng, G.D., Song, B., Liu, Y.Q. and Zhang, C.S. (2008). Predicting the probability distribution of Pb-increased lands in sewage-irrigated region: A case study in Beijing, China. *Geoderma* 147: 192–196.

Yang, Y.R., Liu, X.G., Qu, Y., An, J.L., Jiang, R., Zhang, Y.H., Sun, Y.L., Wu, Z.J., Zhang, F., Xu, W.Q. and Ma, Q.X. (2015a). Characteristics and formation mechanism of continuous hazes in China: A case study during the autumn of 2014 in the North China Plain. *Atmos. Chem. Phys.* 15: 8165–8178.

Yang, Y.R., Liu, X.G., Qu, Y., Wang, J.L., An, J.L., Zhang, Y. and Zhang, F. (2015b). Formation mechanism of continuous extreme haze episodes in the megacity Beijing, China, in January 2013. *Atmos. Res.* 155: 192–203.

Zhang, H.L., Wang, Y.G., Hu, J.L., Ying, Q. and Hu, X.M. (2015a). Relationships between meteorological parameters and criteria air pollutants in three megacities in China. *Environ. Res.* 140: 242–254.

Zhang, L., Wang, T., Lv, M.Y. and Zhang, Q. (2015b). On the severe haze in Beijing during January 2013: Unraveling the effects of meteorological anomalies with WRF-Chem. *Atmos. Environ.* 104: 11–21.

Zhao, B., Wang, S.X., Wang, J.D., Fu, J.S., Liu, T.H., Xu, J.Y., Fu, X. and Hao, J.M. (2013). Impact of national NO_x and SO_2 control policies on particulate matter pollution in China. *Atmos. Environ.* 77: 453–463.

Zhou, Y., Cheng, S., Li, J., Lang, J., Li, L. and Chen, D. (2012). A new statistical modeling and optimization framework for establishing high-resolution PM_{10} emission inventory-II. Integrated air quality simulation and optimization for performance improvement. *Atmos. Environ.* 60: 623–631.

Zhou, Y., Cheng, S., Chen, D., Lang, J., Zhao, B. and Wei, W. (2014a). A new statistical approach for establishing high-resolution emission inventory of primary gaseous air pollutants. *Atmos. Environ.* 94: 392–401.

Zhou, Y., Hammitt, J., Fu, J.S., Gao, Y., Liu, Y. and Levy, J.I. (2014b). Major factors influencing the health impacts from controlling air pollutants with nonlinear chemistry: An application to China. *Risk Anal.* 34: 683–697.

Received for review, January 4, 2017
Revised, March 9, 2017
Accepted, March 23, 2017